



Theoretical and Experimental approach on 2-Benzyloxy-3-Methoxybenzaldehyde (Benzyl-o-vanillin) with Spectroscopic (FT-IR, FT-RAMAN, NMR, UV-VIS), NBO, MEP and Molecular Docking Analysis

K. Manivannane

*Ph.D. Research Scholar (Physics)
A.V.C. College [Autonomous],
Mayladuthurai, (Tamilnadu) [INDIA]
Email: sheelaraj051990@gmail.com*

K. Jayasheela

*Ph. D, Research Scholar (Physics)
Kanchi Mamunivar Center for Post graduate Studies
[Autonomous])
Lawspet (Pondicherry) [INDIA]
Email: sheelaprabha24@gmail.com*

T. Prabhu

*Assistant Professor (Physics)
A.V.C. College [Autonomous],
Mayladuthurai, (Tamilnadu) [INDIA]
Email: ttsprabhu@gmail.com*

Kanchi M

P. B. Nagabala Subramanian

*Assistant Professor (Physics)
Kanchi Mamunivar Center for Post graduate Studies
[Autonomous])
Lawspet (Pondicherry) [INDIA]
Email: EmailID-Required*

ABSTRACT

An anti-proliferative agent 2-benzyloxy-3-methoxy benzaldehyde (Benzyl-o-vanillin) abbreviated as 2B3MB was comprehensively recorded by FT-IR, FT-Raman, UV, as well as ^1H and ^{13}C spectroscopic techniques. The observed absorption and scattering spectral sequence were analyzed to predict the molecular property. The Gaussian computational calculations such as vibrational frequencies, Mulliken and NBO charges, UV-Vis, NMR (GIGO technique) and NLO Properties are carried out by hybrid DFT/B3LYP method with 6-311++G(d,p) basis set. The corresponding results obtained from computational calculations were verified with experimental data. The chemical shifts obtained by GIGO technique were linked to TMS were compared. A detailed study on the electronic and optical properties; absorption wavelengths, excitation energy, dipole moment and frontier molecular orbital energies were carried out. Molecular electrostatic potential (MEP) were generated and tried to predict the

drug activity of the compound by observing FMO interaction profile. The NLO properties related to Polarizability and hyperpolarizability based on the finite-field approach were also discussed.

Keywords:— FT-IR, FT-Raman, NMR, UV analysis, B3LYP, Docking study.

I. INTRODUCTION

Vanillin is a phenolic aldehyde with functional groups aldehyde, ether and phenol. It is an organic solid present in the extracts and essential oils of many plants [1]. Synthetic vanillin is used as a flavoring agent in foods, beverages, and pharmaceuticals. Ortho-Vanillin is a fibrous, light-yellow, crystalline solid. It is a weak inhibitor of protein tyrosinase [2] and displays both anti mutagenic and co-mutagenic properties in Escherichia Coli. O-Vanillin and 2-hydroxybenzaldehyde have been extensively used as precursor to produce coumarin derivatives and neolignane derivatives, which has high

levels of biological activity [3]. It is prepared from the reaction of *o*-vanillin with benzyl bromide in acetone (solvent) and K_2CO_3 (base) in the presence of tetra-*n*-butyl ammonium iodide (catalyst) [4]. It is also used to produce new Azo-Schiff base dyes, possesses moderate antifungal and antibacterial properties [5]. The benzylation process is important in producing new materials such as antioxidants, plastic, rubber and petroleum products [6]. This compound has been reported as a key factor for the synthesis of new anticancer drugs. [7] The crystal structure of the title compound was predicted by the work done by Shafida A. Hamid [8]. Benzyl-*o*-vanillin and benzimidazole nucleus serve as important pharmacophore in drug discovery. It exhibits anti-proliferative activity in HL60 leukemia cancer cells [9].

To the best of our knowledge, the quantum chemical analysis and molecular docking analysis of the titled compound has not been reported so far. Therefore, the present investigation was undertaken to study the structural, vibrational, charge distribution, electronic properties, chemical shifts and NLO properties of the title compound by both experimentally and theoretically. Also, we analyzed the pharmaceutical insights of the molecule by undergone docking schemes.

II. METHODS

Experimental details

The titled compound is purchased from Sigma-Aldrich Chemicals, which is of spectroscopic grade and hence used for recording the spectra as such without any further purification. The FT-IR spectrum of the 2B3MB is recorded in Bruker IFS 66V spectrometer in the range of $4000-400\text{ cm}^{-1}$

with the spectral resolution of $\pm 2\text{ cm}^{-1}$. The FT-Raman spectrum is recorded in the same instrument with FRA 106 Raman module equipped with Nd:YAG laser source operating at $1.064\text{ }\mu\text{m}$ line widths with 200 mW power. The frequencies of all sharp bands are accurate to $\pm 1\text{ cm}^{-1}$. The ^{13}C and ^1H NMR spectra are recorded by high resolution bench top FT-NMR Spectrometer. UV-Visible spectrum was recorded in the range of 200-400 nm, with the scanning interval of 0.2 nm, using the UV-1700 series instrument.

Quantum chemical calculations

The geometry and the vibrational frequencies of the titled compound was first optimized using B3LYP method with 6-311++G (d,p) basis set using Gaussian 09 software [10]. ^1H and ^{13}C NMR chemical shifts were calculated using the GIAO technique. The stability of the optimized geometries was confirmed by getting positive values to all the obtained wavenumbers. VEDA4 program [11] was utilized to calculate the PED, which showed the relative contributions of the redundant internal coordinates to each normal vibrational mode of the molecule and thus enable us numerically to describe the character of each mode. To predict the electronic properties, UV-Visible spectra, NBO and HOMO-LUMO calculations were deliberated using TD-SCF-B3LYP method with same basis set. To envisage the NLO properties of the compound, the dipole moment, linear polarizability and hyperpolarizability were analysed. In addition, the reactive sites of the title compound were identified by plotting MEP surfaces and the changes in the thermodynamic functions (heat capacity, entropy, and enthalpy) were also investigated. The FTIR, FT-Raman vibrational assignments, NMR and MEP surface were graphically viewed using Gauss view 05 package [12].

Molecular Docking Calculations

In order to gain further insights of the molecule, molecular docking study was conducted. The ligand was prepared using DFT/B3LYP/6-311++G(d,p) basis set and stored in PDB file format. Then this ligand was imported into the AutoDock work space and the output for ligand was saved in PDBQT file format. Protein preparation was carried out using the AutoDock Protein preparation wizard. The sugar phosphatase inhibitor activity of the molecule was identified, and the suitable protein was selected for the same. The receptor was taken from the protein data bank (PDB). The PDB ID of the protein CYP2B5 substrate taken for the molecular dynamic simulation study is 2PG5. To satisfy the valency, the polar hydrogens were added, lone pairs were merged to the target protein, Kollman atomic charges were observed and Lamarckian genetic algorithm (LGA) was used. The water molecules were removed from the protein surfaces to mask the surface and the protein file was saved in a PDBQT file format. The receptor grids were generated using 90 Å x 90 Å x 90 Å grid size.

III. RESULT AND DISCUSSION

Conformational Analysis

The optimized geometry of the molecule obtained by B3LYP/6-311++G(d, p) method was used for conformational analysis, which was performed by potential energy surface scan function using PM6 semi empirical method. PM6 method was reported to be faster and reliable compared to other method [13]. The most stable conformer of the bond was obtained by choosing dihedral angle C₄-O₁₃-C₁₄-H₁₇. The selected dihedral angles are varied from 0 to 360° rotation in steps of 10°. A graph was drawn between total energy verses dihedral angle and the same is shown in Figure 1. In

this potential energy curve, the global minimum energy is located at an angle 180° with the energy -805.8791Hartree whereas the maximum energy configuration is obtained for the dihedral angle 240° with the energy value -805.8768Hartree. The energy difference between the maximum and minimum energy conformers characterized by C₄-O₁₃-C₁₄-H₁₇ is 0.023 Hartree, which shows that the change in the dihedral angle does not have much influence in the overall energy of the molecule.

Structural Analysis

The title molecule has 32 atoms with the molecular formula C₁₅H₁₄O₃. The single crystal diffraction study [8] of the title compound predicts that it crystallizes in the monoclinic crystal system, space group P2₁/c, with the crystal cell parameters of a=13.7203 Å, b=4.6599 Å, c=19.1552 Å, V=1213.55 Å³ and Z=4. The minimum energy configuration of the title molecule was again optimized at B3LYP/6-311G++(d, p) level. The optimized structure of the compound is shown in Figure 2 and the optimized structural parameters; bond lengths and bond angles are presented in Table 1. The obtained theoretical data are compared with the data obtained through single crystal X-ray method for the titled molecule reported at the earlier work [4]. From the theoretical values; it is found that most of the optimized bond lengths are slightly larger than the experimental values. Particularly, this variation was seen in the C-C, C-H and C-O bond lengths compared when with experimental ones.

In the case of benzene ring, it is observed that the entire C-H bond in both rings show almost same value (1.085±.005) Å. which indicates that the C-H bond lengths are not subjected to any external influence. But, the C-C bond length varies from 1.381 Å to 1.406 Å. which signifies that, due to the conjugation of electron, the discrimination

between single and double bond is not possible within the rings, whereas the C-C bonds (C₁₉-C₂₇) which connects the two benzene rings, the bond length calculated is 1.502, which shows it's single bonded nature.

In the case of benzyl ring (C₁₀-O₁₂) bond length of aldehyde group is 1.214Å (theoretical) whereas 1.208 Å (experimental) indicates that there is a formation of double bond. In methoxy group (O₁₈-C₁₉ & O₁₃-C₁₄) bond lengths are 1.44 and 1.46Å, which shows single bonded nature.

Bond angles of the carbon atoms in the benzene ring is around 120°. All the angles are varying between 118.9° to 120.6° experimentally and theoretically between 119.5° to 120.6°. Because of the substituted aldehyde group, the aromatic angle C₁-C₂-C₃ is calculated as 119.72°. Due to the presence of the substituted methoxy group, the bond angles C₂-C₃-C₄ and C₃-C₄-C₅ are 119.54° and 119.81° respectively. The bond angles in the aromatic benzene ring, C₂₅-C₂₆-C₂₇ is more elongated (120.6°) and C₂₂-C₂₇-C₂₆ is more contracted (118.9°) indicates that the structure is slightly distorted due to substitutions. The highly stretched bond angle (123.74°) obtained for C₂-C₁₀-O₁₂ in the aldehyde atoms confirms the space charge induction as predicted in the earlier literature [4]. Moreover, the changes in bond angle values indicate that the presence of O atom in the nearby functional groups have considerably changed the hybridization of the carbon atoms. There is the possibility of formation of hydrogen bond between C₁₉-H₂₁-O₁₃ and C₁₀-H₁₁-O₁₈ as predicted in the earlier literature [8] proves that the title compound will serve as an active pharmaceutical and biologically effective candidate.

Atomic charge analysis

The atomic charge analysis plays a substantial role in the quantum chemical calculations which can influence the properties of the molecular system, such as its dipole moment, bond strength, vibrational frequencies, electronic transitions, chemical shifts and molecular polarizability etc. Moreover, these charges are useful in determining the biological activity. The biological activity increases with increasing charge on atom [14]. The atomic charges were calculated by two methods for comparison purpose; Mullikan Population analysis (MPA) and Natural atomic charges (NAC) methods.

Both Mullikan and Natural atomic charges of the title compound were computed by B3LYP/6-311++G(d, p) method and the values are presented in the Table 2. Carbon atoms in the both the benzene rings are expected to be equally negative. This is observed for C₅ and C₆ in the first benzene ring, and for all the five C atoms in the methoxy substituted benzene ring except C₂₇. But in the first benzene, C₁ is observed as slightly positive (0.04) in MPA and slightly negative (-0.15) in NAC. The NAC prediction seems to be valid as the carbon atom is attached only with the H atom, but being close to C₂ which is attached to CHO group, it is reasonable that the reduction in the negative value with respect to the expected value. Thus the MPA prediction is wrong in this case. C₂₇ in the methoxy substituted benzene ring is highly positive (1.15) in MPA and slightly negative (-0.068) in NAC. Here, also the NAC prediction is seeming to be reasonable as C₂₇ atom is attached to the methoxy group, but the O atom lies on the other side of the carbon atom, reflects that it cannot be highly positive. In aldehyde group, as C₁₀ is directly bonded with O atom, the charge is slightly negative (-0.040) in MPA and highly positive (0.412) in NAC. In the case of C₁₄, both the methods predict equally

negative charges (-0.22 and -0.20), guesses that this carbon atom is bonded with three hydrogen atoms from whom it can capture electrons and with one O atom to whom it can donate electron, which results in the occurrence of slightly negative charge distribution. But, in the case of C₁₉, both the methods predict the negative charge on this carbon atom but with unequal magnitudes.

NMR Chemical Shift analysis

Chemical shielding calculations are fast, accurate and applicable for complex systems. The chemical shifts for ¹H and ¹³C atoms of the titled compound were computed for optimized structure, supported by GIAO method. The computed chemical shift values in gas and solvent phase and experimental values at DMSO solvent are presented in Table 3.

¹H NMR spectra

The ¹H NMR spectra (both theoretical and experimental) are shown in Figure 3. The ¹H NMR spectra interpreted significantly in an attempt to measure the possible different effects appearing on the chemical shift values of proton. [17] The usual scale, for PMR (Proton Nuclear Magnetic resonance) studies is about 10ppm. In the present study, all the theoretical HNMR chemical shift values are in good agreement with experimental values. HNMR chemical shifts in the ligand ring protons i.e., for H₇, H₈, H₉, d = 7.30, 7.27 & 7.29 ppm respectively while for the benzyl ring protons (H₂₈, H₂₉, H₃₀, H₃₁, H₃₂), the experimentally observed values are at d = 7.23, 7.26, 7.17, 7.10 & 7.08 respectively. All these values are within the expected range of aromatic chemical shift of HNMR. The ¹H NMR spectrum shows the chemical shift of the aldehydic proton is at d= 10.14 ppm for H₁₁ atom due to the strong intermolecular OH bonding. In O-CH₃ group, it is observed at 3.85 (H₁₆) and 5.09 (H₁₇, H₁₅) ppm while

for O-CH₂, it is observed at 4.6 (H₂₀) and 4.9 (H₂₁) ppm.

¹³C NMR spectra

The ¹³C NMR spectra (both theoretical and experimental) are shown in Figure 4. The titled compound showed the chemical shifts of carbon atoms in benzene rings as well as in aldehyde and methoxy groups. This chemical shift values for aromatic ring carbon atoms are expected between 120 - 130 ppm: around 120 in gas phase and 130 in solvent phase [11]. This trend has been observed in the case of C₅ and C₆ in the first benzene ring and the carbon atoms in the ligand structure (C₂₂ – C₂₆) the values are around 130ppm. These observations also confirmed with the charge analysis where all these carbon atoms were found to have almost equal negative charges around 0.2 Coulomb. In DMSO, the peak appears at d = 190.37 ppm in the ¹³C NMR spectrum of C₁₀ was assigned to the aldehyde C=O group while the value theoretically obtained at 177.15 ppm. This value is well agreed with the experimental value obtained in the earlier literature [15]. The presence of O atom, makes the carbon value very greater than that of aromatic carbons. This is also in line with the charge analysis where this carbon atom was found to have extremely positive charge (0.42Coulomb). The carbon atoms at methoxy groups C₁₄ (OCH₃) and C₁₉ (OCH₂) have experimental lower values (56.19 ppm and 77.47 ppm) respectively which is well coincide with the values predicted in the earlier literature [16] at 56.16 & 71.16 ppm. The difference in the chemical shift value between C₁₉ and C₁₄ are due to the presence of number of H atoms in their atmosphere. Due to the presence of O atom in these methoxy group, these observed experimental values are relatively higher when compared to that of normal methyl carbon atom (30 ppm) moiety. The experimentally observed carbon signals in DMSO at d = 128.78,

136.45, 153.14, 151.13, 130.40 & 128.78 ppm for C₁, C₂, C₃, C₄, C₅ & C₆ respectively while other aromatic carbon signals of benzyl ring were observed at

Vibrational Investigation

The titled molecule under investigation has 32 atoms and has 90 normal modes of fundamental vibrations. Vibrational wave numbers for all the fundamental modes of the titled compound were computed using DFT (B3LYP) methods with 6-311++G (d, p) basis set and the values along with the experimental values are presented in Table 4. The experimental and theoretical spectra of the titled compound are shown in Figure 5 and 6, respectively.

By observing the experimental and theoretical frequencies, the theoretical values were slightly higher than the experimental values for the majority of the normal modes, comes to the conclusion that two factors may be responsible for the discrepancies between the experimental and computed wave numbers; the first is caused by the unpredictable electronic distribution among the different bonds in the molecule and the second reason is the anharmonic nature of the vibrations which cannot be accounted completely by the theory. To make coincidence with experimental and theoretical data, scaling strategies were utilized.

CH vibration

The experimental frequencies for aromatic C-H stretching vibrations and aliphatic C-H stretching vibrations are observed at 3092, 3086, 3064, 3048, 3000, 2974, 2963, 2941 & 2841 cm⁻¹ in FTIR and 3079, 3062, 3054, 3042, 3006 & 2836 cm⁻¹ in FT-RAMAN respectively. In the present study, there are eight C-H stretching vibrations observed for the aromatic rings within the expected

range of 3100 – 3000 cm⁻¹ i.e., at 3086, 3079, 3077, 3069, 3064, 3061, 3051 and 3048 cm⁻¹ respectively. The C-H stretching modes usually appear with strong Raman intensity due to their high polarization. As we know, aliphatic C-H stretching occurs in the region of 3000-2850 cm⁻¹, the theoretically observed six aliphatic C-H stretching vibrations at 3021, 2981, 2980, 2919, 2911 and 2866 cm⁻¹ in this study confirms the same.

The C-H in-plane bending mode usually occurs as strong to weak bands in the region of 1300 to 1200 cm⁻¹ while the C-H out of plane bending vibrations are expected to be occur as a strong to weak intensity bands in the region of 1000-600 cm⁻¹ [18]. The bands due to C-H in-plane ring vibration interacting with C-C stretching vibrations and are observed as a number of m-w intensity sharp bands in the region 1000–1300 cm⁻¹ which reflects the characteristics of the molecule. Experimental study of the title compound manifested its C-H in-plane bending vibrations at 1313 and 1213 cm⁻¹ in the FT-Raman spectrum though theoretically it appears at 1368, 1162cm⁻¹ for the same with PED contribution of ~35%. The C-H out-of-plane bending vibrational frequencies depends on the number of adjacent hydrogen atoms on the ring system, but they are not significantly affected by the nature of the substituents. The recorded FT-IR spectrum of the titled molecule showed bands at 653 and 970 cm⁻¹ while its FT-Raman spectrum, manifested bands at 963 and 719 cm⁻¹ which were assigned to the C-H out-of-plane bending vibrations. Their corresponding computed values were noted at 965, 837, 815 and 703 cm⁻¹ respectively, with PED contribution of 50%.

C=O vibration

The stretching mode of carbonyl (C=O) group of the aldehyde moiety is expected in

the range of 1740 to 1720 cm^{-1} . Theoretical study of the titled molecule showed only one C=O stretching band at 1691 cm^{-1} with PED contribution of 88%. Slight deviations in this may be due to the conjugation of hydrogen bond. Experimentally, in both FT-IR and FT-Raman spectra it is observed at 1693 and 1691 cm^{-1} respectively. The C=O in-plane and out-of-plane bending modes are expected in the region 625 ± 70 and 540 ± 80 cm^{-1} respectively [19]. The theoretically calculated wave number for the C=O in-plane bending mode of the title compound appeared at 634 cm^{-1} with PED contribution of 10% while in the FT-IR spectrum it appeared at 660 cm^{-1} . The C=O out-of-plane bending vibration falls within the expected range.

C-O vibration

In C-O group, the absorption is sensitive for both the carbon and oxygen atoms. Normally the C–O stretching vibration occurs in the region 1000-1260 cm^{-1} . The intensity of the carbonyl group increases, due to the conjugation (or) formation of hydrogen bonds [20]. The increase in conjugation, which increase the intensity of Raman lines as well as the IR band intensities. According to the above facts, there are four theoretical wave numbers were observed at 1234, 1222, 1010 and 902 cm^{-1} . Corresponding experimental FT-IR bands were observed at 1248, 1179 and 962 cm^{-1} . In experimental FT-RAMAN it was observed at 1248, 1197 and 1064 cm^{-1} . The in-plane bending vibrations of $\beta_{\text{C-O}}$ are observed at 699 cm^{-1} in FT-IR spectrum and at 725 cm^{-1} in B3LYP method.

C-C vibration

The CC stretching vibrations are very much important in the spectrum of benzene and its derivatives. It is generally observed between 1600 to 1400 cm^{-1} , in which the band between 1500-1600 cm^{-1} assigned to C-

C stretching and 1400-1500 cm^{-1} to C=C stretching. In the present compound there are twelve CC stretching vibrations were observed at 1589, 1569, 1566, 1559, 1475, 1464, 1454, 1448, 1437, 1432, 1425 and 1415 cm^{-1} by B3LYP/6-311++(d, p) method. In experimental recorded spectrum, they are assigned at 1601, 1592, 1585, 1480, 1455 and 1446 cm^{-1} in FTIR and 1599, 1587, 1586, 1491, 1476, 1456, 1452, 1441, 1440, 1426 and 1414 cm^{-1} in FT-RAMAN respectively. All CC vibrations in the benzene rings were within the expected range. The C-C bending modes are appeared as mixed modes with C-H vibrations.

UV-Visible study

The UV-Vis absorption spectrum of the titled compound is recorded in the range 200-800 nm are shown in Figure 7. Theoretical calculations have been investigated in Gas phase and in organic solvent (ethanol) by TD-DFT method in order to get a deeper insight into the possible electronic excitations, wavelengths, oscillator strengths and major orbital contributions of various excitations of the titled compound. The electronic transitions and the corresponding excitation energies for these two phases are presented Table 5. The calculated absorption maxima values are at 335.45, 297.15 and 264.5 nm for gas phase and for ethanol it was 340.09, 307.55 and 275.53 nm. The experimental absorption maxima is obtained at 306.10 nm.

The energy gap between HOMO and LUMO is used to find the chemical behavior, high reactivity, low kinetic stability of the compound. Using B3LYP method, the calculated HOMO and LUMO energies of the titled molecule is -0.2555 and -0.7778eV, respectively, and the energy gap between them is 0.1777 eV. The HOMO-LUMO energy gap and different

reactivity descriptors of molecule in both levels are presented in Table 6. The negative surface was represented as red and the positive charges were represented by green color. It showed the spread of HOMO over the aldehyde substituted benzene ring and some parts of the second ring while LUMO was located only on the benzaldehyde. The low HOMO-LUMO energy gap reveals the ultimate possible charge transfer within the molecule and hence there is the possibility of high chemical and biological reactivity [20]. With respect to the electronic transitions, there are three maximum computed wavelengths at 340.09, 307.55 and 275.53 nm, which correspond to the contribution of HOMO/LUMO (70%), H-1/L(94%), H-2/L (51%) in the solvent phase. These transitions can be accounted for non-bonding transition ($n \rightarrow \pi^*$) of the lone pair in the molecule are shown in Figure 8.

NBO Analysis

The bonding and non-bonding (anti-bonding) interactions can be quantitatively described in terms of the NBO analysis and is tabulated in Table.7. In this study, the charges transferring from bonding to anti-bonding levels were analyzed. The intramolecular hyper conjugative interactions are caused by the orbital overlapping between σ and π (C-C, C-O, C-H, O-H) bond orbitals. These interactions are observed as increase in electron density (ED) in C-C, C-O, C-H and O-H anti bonding orbitals which that makes weakness in the respective bonds and twelve transitions are took place. The highest stabilization energy of the title molecule are C₁-C₆ to C₄-C₅ ($\pi - \pi^*$, 22.02 kcal/mol), C₄-C₅ to C₂-C₃ ($\pi - \pi^*$, 21.69 kcal/mol), O₁₂ to C₁₀-H₁₁ ($n - \sigma^*$, 21.54 kcal/mol), C₂₂-C₂₃ to C₂₆-C₂₇ ($\pi - \pi^*$, 20.71 kcal/mol), C₂₄-C₂₅ to C₂₆-C₂₇ ($\pi - \pi^*$, 20.7 kcal/mol), C₂₂-C₂₃ to C₂₄-C₂₅ ($\pi - \pi^*$, 20.65 kcal/mol), C₂₆-C₂₇ to C₂₂-C₂₃ ($\pi - \pi^*$, 20.38 kcal/

mol), C₂₆-C₂₇ to C₂₄-C₂₅ ($\pi - \pi^*$, 20.15 kcal/mol), C₁-C₆ to C₄-C₅ ($\pi - \pi^*$, 20.02 kcal/mol), C₂₄-C₂₅ to C₂₂-C₂₃ ($\pi - \pi^*$, 19.71 kcal/mol), C₂-C₃ to C₁-C₆ ($\pi - \pi^*$, 19.43 kcal/mol), C₁-C₆ to C₂-C₃ ($\pi - \pi^*$, 18.72 kcal/mol), C₂-C₃ to C₄-C₅ ($\pi - \pi^*$, 18.55 kcal/mol), C₂-C₃ to C₁₀-O₁₂ ($\pi - \pi^*$, 18.37 kcal/mol), O₁₂ To C₂-C₁₀ ($\pi - \pi^*$, 18.09 kcal/mol) and C₄-C₅ to C₁-C₆ ($\pi - \pi^*$, 17.05 kcal/mol).

Molecular Electrostatic Potential (MEP) Analysis

The MEP map for 2B3MB molecule is as shown in Figure 9 and the different values of MEP surface are represented by different colors: red, blue and green which indicates the regions of most negative, most positive and zero electrostatic potential, respectively. it is evident that the maximum negative region (electrophilic) shown in red color at the C=O site is the strongest affinity for a proton while the maximum positive region (nucleophilic) referred in - blue color around the hydrogen atoms is the strongest affinity for electron. The positive and negative potential of the molecule ranges from -5.311×10^{-2} au. to $+5.311 \times 10^{-2}$ au.

Molecular Docking

The study of molecular docking of the present molecule was carried out by Auto Dock – Vina software and PyMol molecular graphics system [21]. The legend was chosen by minimizing its energy at B3LYP/6-311G++ (d, p) functional and basis sets and the online tool “Pass” is used to predict the different types of biological activities of the title molecule. In this present study, Protein name CYP2B5 substrate (protein ID: 2PG5). Generally, Hydrogen were added with target protein and therefore Kollman atomic charges were observed and Lamarckian genetic algorithm (LGA) was used for molecular docking study in Auto Dock software package. The binding pocket of protein was obtained by grid size of 92

X, 92 Y & 92 Z Å with the help of Auto grid. By using Auto dock software, the inhibition constants, intermolecular energy are calculated. The bond distance of the title molecule to the targeted protein were 2.0, 2.1 and 3.2 with inhibition constant of three residue (THR 'A') involved in bonding with the title compound were obtained using Discover studio visualizer 4.1 software and the values are tabulated in Table 8. The formation of hydrogen between legends and protein were represented by yellow dotted lines in the Figure 10. In addition, the molecule is suggested with hydrophobic activity which is consistent with the experimental values.

IV. FIGURES AND TABLES

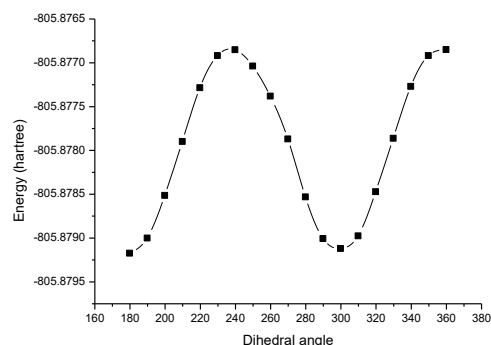


Figure 1. Potential energy scan of 2-benzyloxy-3-methoxy benzaldehyde

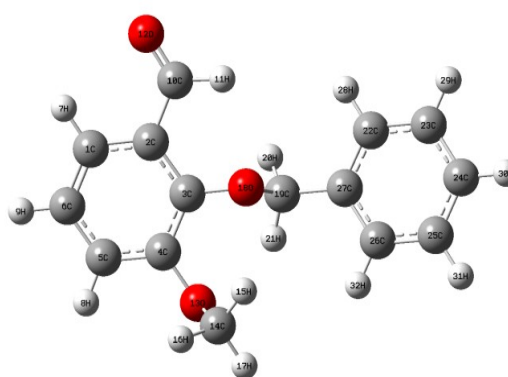


Figure 2: Optimized structure of 2-benzyloxy-3-methoxy benzaldehyde

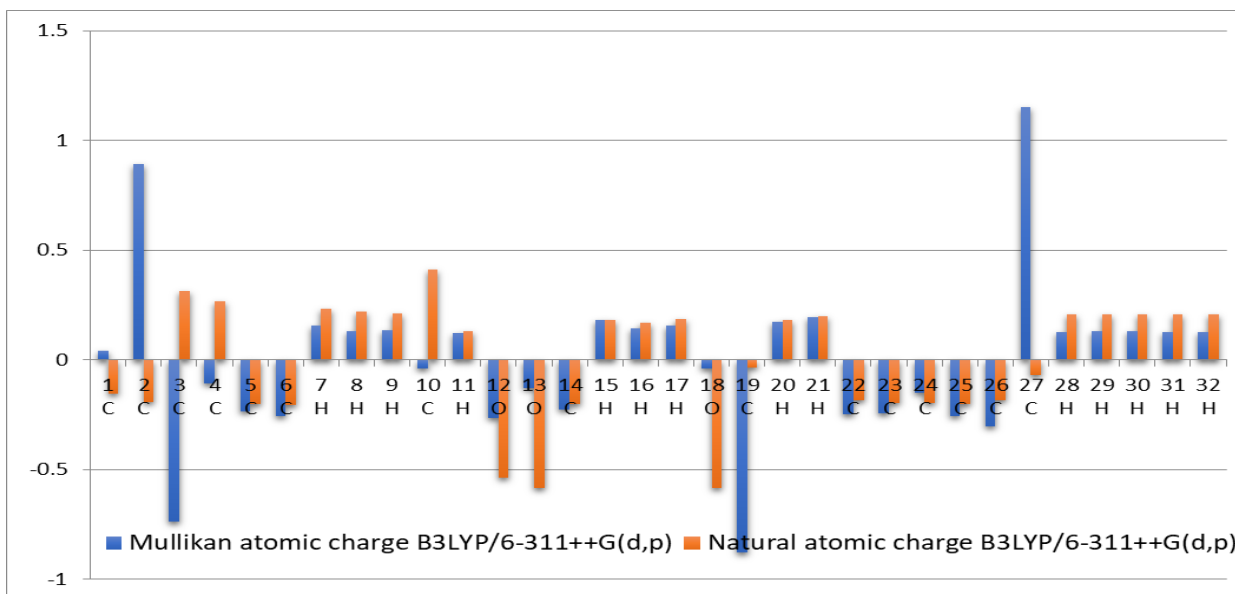


Figure 3: Mullikan and Natural charge analysis of 2-benzyloxy-3-methoxy benzaldehyde

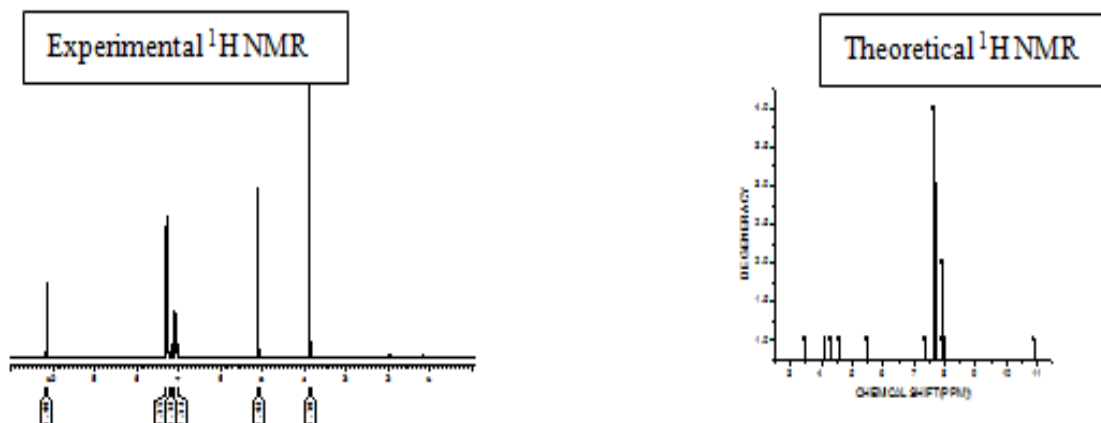


Figure 4: Experimental and Theoretical ^1H NMR spectra of 2-benzyloxy-3-methoxy benzaldehyde

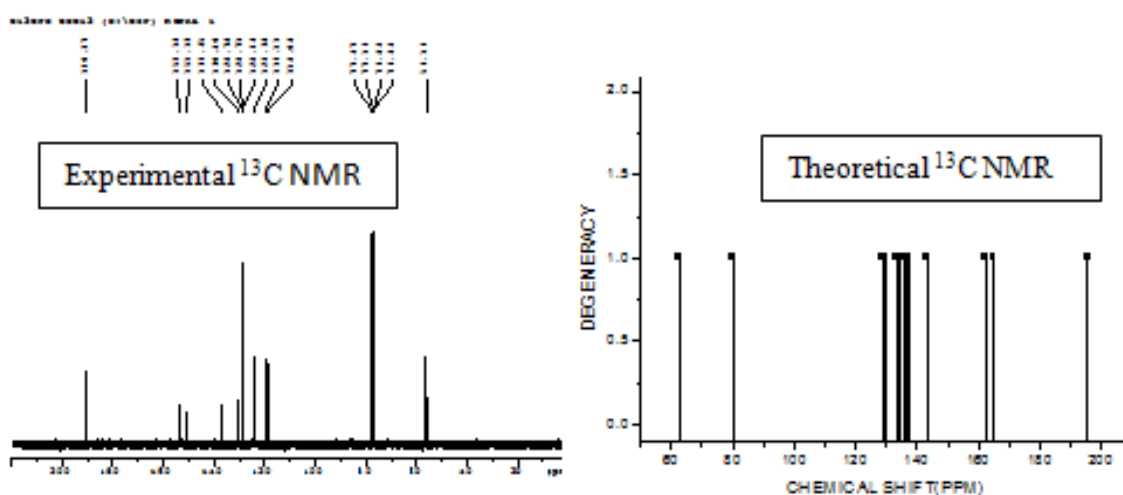


Figure 5: Experimental and Theoretical ^{13}C NMR spectra of 2-benzyloxy-3-methoxy benzaldehyde

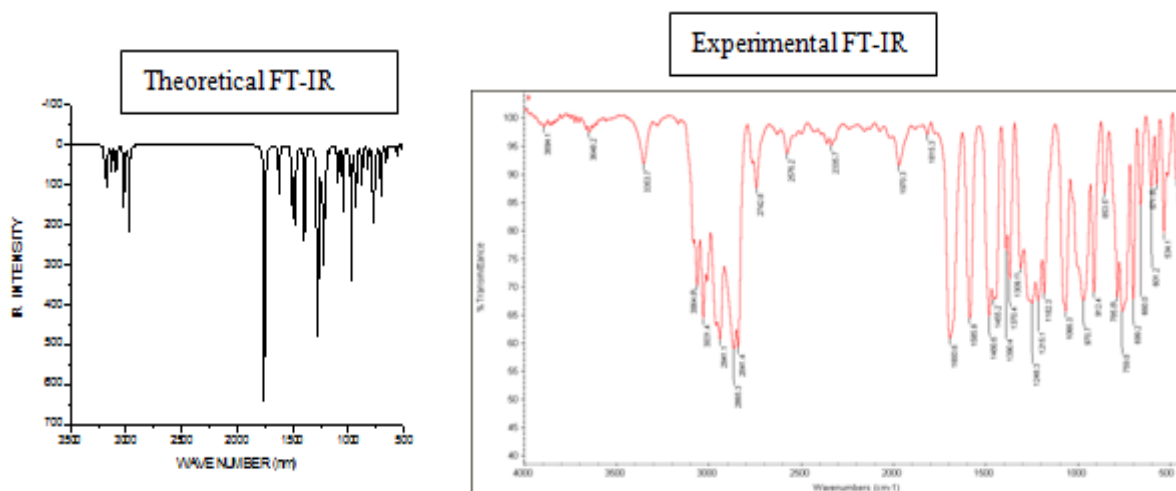


Figure 6: Theoretical and Experimental FT-IR vibrational frequencies spectra of 2-benzyloxy-3-methoxy benzaldehyde

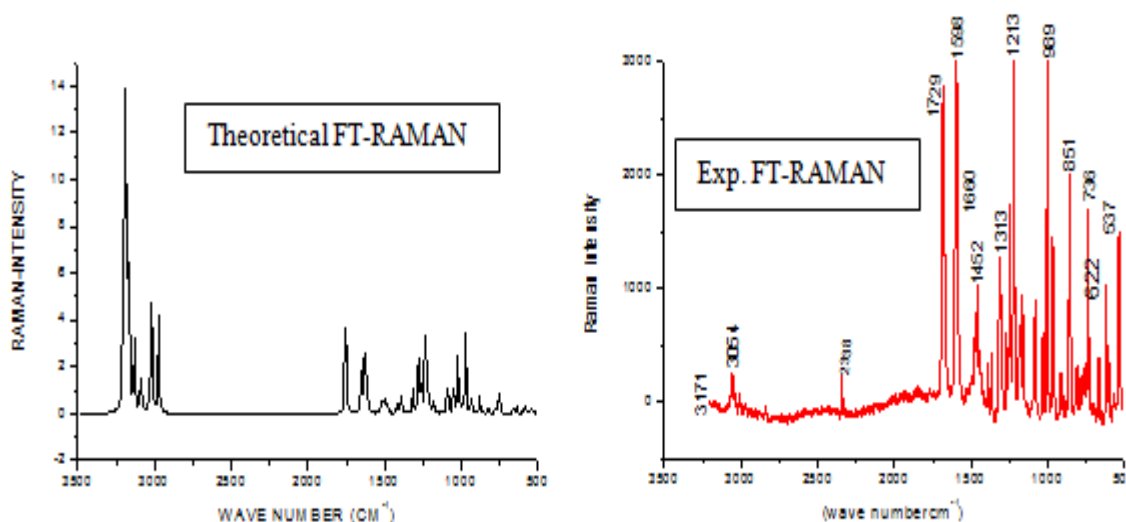


Figure 7: Theoretical and Experimental FT-RAMAN vibrational frequencies spectra of 2-benzyloxy-3-methoxy benzaldehyde

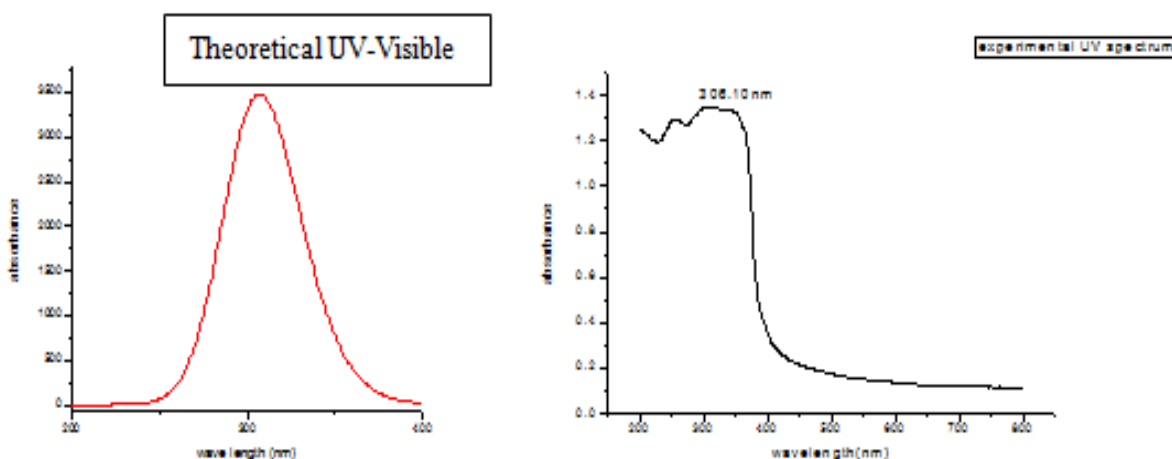


Figure 8: Experimental and Theoretical and UV-Vis Spectra of 2-benzyloxy-3-methoxy benzaldehyde

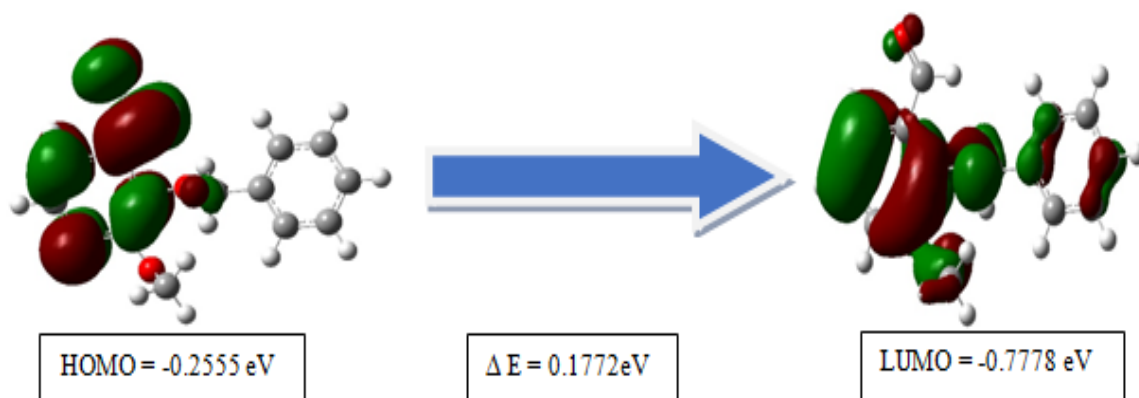


Figure 9: Frontier molecular orbitals of 2-benzyloxy-3-methoxy benzaldehyde

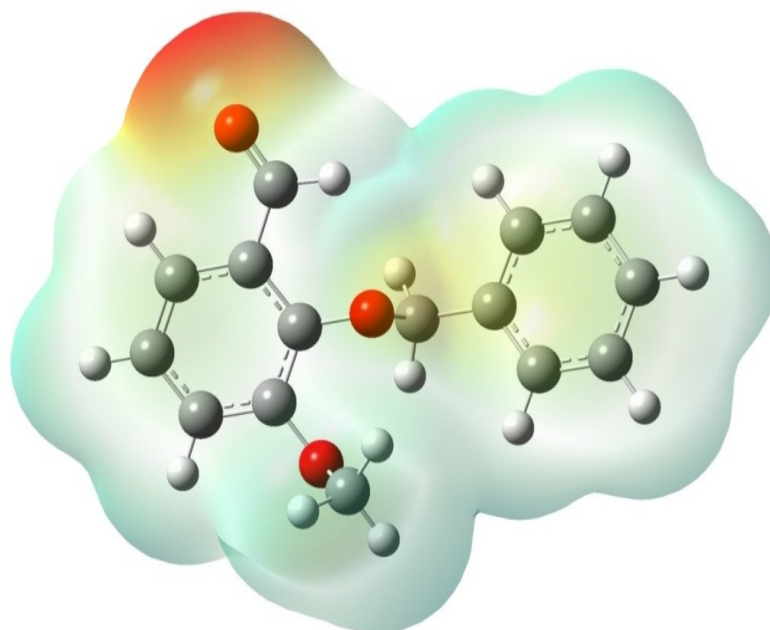


Figure 10: Molecular electrostatic potential of 2-benzyloxy-3-methoxy benzaldehyde

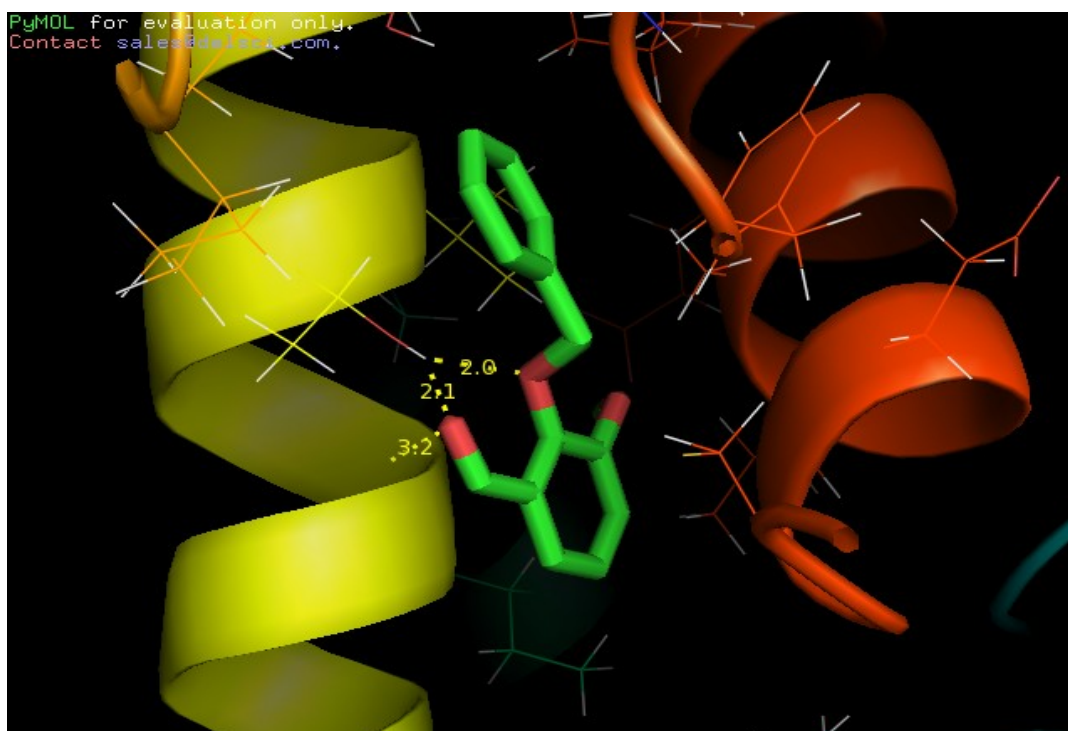


Figure 11: Molecular binding pose of 2-benzyloxy-3-methoxy benzaldehyde

Table 1: Optimized Geometrical parameter for 2-benzyloxy-3-methoxy benzaldehyde Computed at B3LPY/6-311++G(d,p).

Geometrical parameters	Bond length in Å		Geometrical parameters	Bond angle in degree	
	6311++G(d,p)	XRD		6311++G(d,p)	XRD
C1-C2	1.4027	1.404	C2-C1-C6	120.44	119.7
C1-C6	1.3859	1.376	C2-C1-H7	118.01	122.2
C1-H7	1.0834	0.970	C2-C1-H7	121.54	120.0
C2-C3	1.4058	1.395	C1-C2-C3	119.72	119.8
C2-C10	1.4835	1.485	C1-C2-C10	119.65	120.1
C3-C4	1.4065	1.409	C3-C2-C10	120.62	120.1
C3-O18	1.3724	1.374	C2-C3-C4	119.54	119.9
C4-C5	1.3913	1.384	C2-C3-O18	120.06	119.2
C4-O13	1.3758	1.365	C4-C3-O18	120.34	120.7
C5-C6	1.3971	1.395	C3-C4-C5	119.81	119.6
C5-H8	1.0841	0.955	C3-C4-O13	120.62	115.7
C6-H9	1.0836	1.043	C5-C4-O13	119.52	124.7
C10-H11	1.1033	0.984	C4-C5-C6	120.60	120.1
C10-O12	1.2138	1.208	C4-C5-H8	118.19	119.5
O13-C14	1.4368	1.428	C6-C5-H8	121.19	120.4
C14-H15	1.0927	0.961	C1-C6-C5	119.83	120.9
C14-H16	1.0949	0.959	C1-C6-H9	120.37	121.4
C14-H17	1.0895	0.960	C5-C6-H9	119.79	117.7
O18-C19	1.4583	1.457	C2-C10-H11	115.44	115.7
C19-H20	1.0954	1.004	C2-C10-O12	123.74	123.1
C19-H21	1.0921	1.009	H11-C10-O12	120.81	121.1
C19-C27	1.5023	1.494	C4-O13-C14	114.75	116.8
C22-C23	1.3927	1.388	O13-C14-H15	111.03	109.4
C22-C27	1.3983	1.393	O13-C14-H16	110.38	109.5
C22-H28	1.0852	0.936	O13-C14-H17	106.16	109.5
C23-C24	1.3944	1.390	H15-C14-H16	109.85	109.5
C23-H29	1.0841	0.983	H15-C14-H17	109.93	109.5
C24-C25	1.3939	1.387	H16-C14-H17	109.39	109.5
C24-H30	1.0842	0.996	C3-O18-C19	115.02	115.2
C25-C26	1.3934	1.392	O18-C19-H20	108.04	108.2
C25-H31	1.0842	0.937	O18-C19-H21	108.89	110.7
C26-C27	1.3978	1.393	O18-C19-C27	108.53	106.1
C26-H32	1.0815	0.977	H20-C19-H21	109.00	108.5
			H20-C19-C27	110.96	113.3
			H21-C19-C27	111.32	110.1
			C23-C22-C27	120.62	120.6
			C23-C22-H28	119.80	119.5
			C27-C22-H28	119.57	119.9
			C22-C23-C24	119.99	119.9
			C22-C23-H29	119.90	118.0

Table 2: Atomic Charges of 2-benzyloxy-3-methoxy benzaldehyde with B3LYP/6-311++G (d,p) basis set.

Atoms	Mullikan atomic charge B3LYP/6-311++G(d,p)	Natural atomic charge B3LYP/6-311++G(d,p)
1 C	0.04017	-0.15413
2 C	0.89312	-0.19301
3 C	-0.73751	0.31414
4 C	-0.10791	0.26448
5 C	-0.23471	-0.20087
6 C	-0.25531	-0.20761
7 H	0.15411	0.23055
8 H	0.13111	0.22068
9 H	0.13378	0.21226
10 C	-0.04021	0.41243
11 H	0.12365	0.12912
12 O	-0.26511	-0.53614
13 O	-0.13011	-0.58336
14 C	-0.22667	-0.20259
15 H	0.17986	0.18243
16 H	0.14111	0.16825
17H	0.15596	0.18421
18 O	-0.04031	-0.58646
19 C	-0.87921	-0.03655
20 H	0.17248	0.17956
21 H	0.19418	0.19726
22 C	-0.24724	-0.18288
23 C	-0.24541	-0.19918
24 C	-0.15003	-0.19575
25 C	-0.25658	-0.20074
26 C	-0.30349	-0.18558
27 C	1.15358	-0.06833
28 H	0.12501	0.20702
29 H	0.13020	0.20865
30 H	0.12922	0.20791
31 H	0.12783	0.20749
32 H	0.12751	0.20673

Table 3: Calculated ^1H and ^{13}C NMR Chemical shifts (ppm) of 2-benzyloxy-3-methoxy benzaldehyde

Atom	Gas	CdCl ₃	Exp.	Atom	Gas	CdCl ₃	Exp.
Benzene ring							
C1	129.13	128.62	128.78	H7	8.13	8.02	7.30
C2	137.14	136.19	136.45	H9	7.63	7.36	7.29
C3	165.08	164.86	153.14	H8	7.35	7.67	7.27
C4	162.44	162.49	151.13	H28	7.92	7.93	7.23
C5	135.46	137.10	130.40	H29	7.72	7.69	7.26
C6	129.13	129.52	128.78	H30	7.67	7.67	7.17
C22	136.91	137.01	136.40	H31	7.72	7.72	7.10
C23	133.19	133.56	130.40	H32	7.93	7.93	7.08
C24	133.41	134.24	128.78				
C25	133.16	133.46	130.40				
C26	136.13	136.36	128.78				
C27	143.04	143.13	136.40				
Ligand							
C10	177.15	195.61	190.37	H11	10.89	10.88	10.14
C14	63.041	62.58	56.19	H16	3.48	3.48	3.85
C19	80.791	80.12	77.47	H17	4.13	4.13	5.09
				H15	4.32	4.32	5.09
				H20	4.56	4.56	4.6
				21H	5.50	5.50	4.9

Table 4: Experimental and calculated vibrational frequencies value of 2-benzyloxy-3-methoxy benzaldehyde

No. of Modes	Observed Frequencies		B3LYP/6-311++G(d,p)		PED%
	FT-IR	FT-RAMAN	Unscaled	Scaled	
1.	3092		3198.61	3086.65	vCH(91)
2.	3086	3079	3190.91	3079.23	vCH(91)
3.	3064	3062	3189.29	3077.675	vCH(100)
4.		3054	3180.82	3069.49	vCH(101)
5.	3048	3042	3175.64	3064.49	vCH(91)
6.	3031		3171.75	3060.74	vCH(89)
7.	3027		3162.32	3051.64	vCH(91)
8.	3018		3159.57	3048.99	vCH(99)
9.	3000	3006	3130.56	3020.99	vCH(97)
10.	2974		3088.78	2980.67	vCH(89)
11.		2968	3087.72	2979.65	vCH(86)
12.	2963		3024.41	2918.55	vCH(100)
13.	2941		3016.71	2911.13	vCH(100)
14.	2841	2836	2970.88	2866.90	vCH(100)
15.	1693	1691	1752.82	1691.47	vCO (88)
16.	1601	1598	1646.78	1589.14	vCC(36) β CC (11)
17.	1592	1587	1626.74	1569.80	vCC(60) β CC (14)
18.		1586	1623.82	1566.98	vCC(57) β CC(12)
19.	1585	1491	1615.6	1559.05	vCC(51) β CC(12)
20.	1480	1476	1529.49	1475.96	vCC(88) β CH(68) β CC (11)
21.		1464	1518.06	1464.93	vCC(78) β CH(74) τ HCOC(12)
22.	1455	1456	1507.71	1454.94	vCC (67) β CH(74) γ CHO(14)
23.	1450	1452	1501.00	1448.47	vCC(66) β CH(32)
24.	1446	1441	1489.69	1437.55	vCC(54) β CH(80)
25.		1440	1484.55	1432.59	vCC(20) β HCH(46)
26.		1426	1476.97	1425.28	vCC(22) β HCH (18)
27.		1414	1466.72	1415.39	vCC (68) τ CHHH(70)
28.	1390		1417.87	1368.25	β CO(32) τ HCOC(12)
29.		1317	1392.34	1343.61	β CO(26) τ HCOC(38)
30.	1309	1309	1359.07	1311.50	vCC(68)

No. of Modes	Observed Frequencies		B3LYP/6-311++G(d,p)		PED%
	FT-IR	FT-RAMAN	Unscaled	Scaled	
31.		1271	1343.29	1296.27	vCC(73)
32.		1239	1316.48	1270.40	vCC(77)
33.	1248	1248	1279.36	1234.58	vCC(10)vOC(33) β HCC(18)
34.	1215		1262.18	1218.04	vCC(34) β HCC(25)
35.		1213	1244.46	1200.90	β CO(68)
36.	1208	1202	1236.84	1193.55	vCC(39) β CCC(18)
37.	1193	1197	1222.75	1179.95	vOC(34) vCC(11) γ CHOH(12)
38.	1182	1185	1204.8	1162.63	β CH(10) γ CHOH(51)
39.		1179	1201.86	1159.79	β HCC(71)
40.		1170	1183.19	1141.77	β CC(96)
41.	1151	1156	1181.81	1140.44	vCC(12) β HCC(52)
42.		1115	1169.26	1128.33	β CO(88)
43.		1110	1109.55	1070.71	vCC(21) β HCC(32)
44.		1087	1089.77	1051.62	vCC(46) β HCC(36)
45.	1066		1049.87	1013.12	vCC(34) β HCC(20)
46.		1064	1047.16	1010.51	vOC(58)
47.		1023	1032.95	996.79	τ CCOH(86)
48.		1018	1018.87	983.21	β CC(24) β HCC(58)
49.		995	1008.25	972.96	β CC(34)
50.		989	998.01	963.08	β CC
51.		972	990.29	955.63	β CC(13) τ HCOC(55)
52.	970		987.13	952.58	τ HCCH(42) τ HCCC(46)
53.	962		973.7	939.62	vOC(56)
54.		926	944.71	911.64	τ CCCH(73)
55.	912		935.22	902.48	vOC(11) τ HCCH(42) τ HCCC(24)
56.		902	929.39	896.86	vOC(24) β CC(17)
57.			877.44	846.72	β CCC(13) β CCO(13)
58.		851	857.73	827.70	τ HCCC(99)
59.	853		828.15	799.16	β CCC(24)
60.	785		820.05	791.34	τ CCCH(28) τ HCCH(12)

No. of Modes	Observed Frequencies		B3LYP/6-311++G(d,p)		PED%
	FT-IR	FT-RAMAN	Unscaled	Scaled	
61.	759		777.31	750.10	ν CC(15) β CCO(19)
62.		736	775.02	747.89	τ CCCH(17) τ CCCC(15)
63.	699		752.06	725.73	β CCO(10) τ CCCC(15)
64.		695	709.24	684.41	τ HCCC(15) τ CCCC(15)
65.	660		657.1	634.10	β CO(10)
66.		622	635.94	613.68	β CH(71)
67.	601	607	604.99	583.81	β CH
68.	594		583.49	563.06	β CH(18) β CCO(11)
69.	571	576	565.99	546.18	τ CCC(33) τ CCCO(10)
70.		538	543.74	524.70	β CCC(10) β CCO(12) τ CCCC(12)
71.	534	530	503.76	486.12	β CC(16) γ CCCC(12)
72.	465	467	467.62	451.25	β CC(10)
73.		405	413.34	398.87	τ CCCC(90)
74.		394	394.83	381.01	β CC(10) β CCO(33)
75.		364	369.81	356.86	β OC(12) τ CCCO(24)
76.		349	350.76	338.48	β CO(21) τ CCC(37)
77.		322	324.77	313.40	β CO(13) τ CCC(32)
78.		274	276.86	267.16	β CO(11) τ CCCC(20)
79.		258	259.49	250.40	β CC(12)
80.		207	209.78	202.43	β CC(25) τ CCCC(34)
81.		183	188.03	181.44	β CC(14) τ HCO(17) τ CCCC(21)
82.		163	167.06	161.21	β CO(10) τ HCO(60)
83.		157	157.43	151.92	β OC(12) τ CCCO(57)
84.		122	125.9	121.49	τ CCO(51)
85.		83.05	85.93	82.92	β CO(10) τ CCO(16) τ CCOC(12) γ CCCC(11)
86.		70	74.49	71.88	τ CCOC(75)
87.		58	60.78	58.65	τ CCCO(14) τ CCOC(56)
88.		48	52.41	50.57	τ COC(25) τ CCO(16) τ CCCO(28)
89.		23	25.23	24.34	τ COCC(24) τ CCCO(64)
90.		17	17.93	17.30	τ COCC(59) τ CCCO(26)

ν -stretching; β -in-plane bending; δ -deformation; γ -out of plane bending; ω -wagging and τ -torsion.

Table 5: Theoretical electronic absorption spectra of 2-benzyloxy-3-methoxy benzaldehyde (absorption wavelength λ (nm)), excitation energies E (ev) and oscillator strengths (f) using TD-DFT/B3LYP/6-311++G(d,p) method.

λ (nm)		E(eV)	(f)	Major contribution
Theoretical	Experimental			
353.45		3.5078	0.0001	H-1->LUMO (92%)
297.15		4.1725	0.0670	HOMO->LUMO (91%), H-4->L+3 (2%)
264.50		4.6875	0.0056	H-2->LUMO (79%), H-5->LUMO (5%), H-4->LUMO (6%), H-3->LUMO (9%)
340.09		3.6456	0.0002	H-3->LUMO (70%), H-1->LUMO (13%)
307.55	306.10	4.0313	0.0848	HOMO->LUMO (94%)
275.53		4.4998	0.0043	H-2->LUMO (51%), H-1->LUMO (40%)

Table 6: Homo, LUMO, Kubo gap, global electronegativity, global hardness and softness, global electrophilicity index of 2-benzyloxy-3-methoxy benzaldehyde

Parameters	Gas
E_{HOMO} (ev)	-0.25550
E_{LUMO} (ev)	-0.07778
$\Delta E_{HOMO-LUMO}$ gap (ev)	-0.17772
Electronegativity (χ) (ev)	0.16664
Global hardness (η)(ev)	0.08886
Global softness (S)(ev)	0.35544
Electrophilicity index (ω)(ev)	0.15625
Dipole Moment (m) (debye)	3.8606

Table 7: Second order perturbation theory of Fock matrix in NBO basis of 2-benzyloxy-3-methoxy benzaldehyde

Donors	Type of Bonds	Occupancy	Acceptors	Type of Bonds	Occupancy	Energy E(2) Kcal/mol	Energy Difference E(j)-E(i) a.u.	Polarized Energy F(i,j) a.u.
C 1 - C 2	σ	1.97150	C 2 - C 3	σ^*	0.03265	3.59	1.25	0.06
C 1 - C 2	σ	1.97150	C 3 - O 18	σ^*	0.02624	3.93	1.05	0.057
C 1 - C 6	π	1.67057	C 2 - C 3	σ^*	0.40550	18.72	0.28	0.065
C 1 - C 6	π	1.67057	C 4 - C 5	π^*	0.34593	22.02	0.28	0.07
C 1 - H 7	σ	1.97799	C 2 - C 3	σ^*	0.03265	4.57	1.07	0.063
C 1 - H 7	σ	1.97799	C 5 - C 6	σ^*	0.01491	3.73	1.08	0.057
C 2 - C 3	σ	1.97281	C 1 - C 2	σ^*	0.02157	3.7	1.28	0.061
C 2 - C 3	π	1.64062	C 1 - C 6	π^*	0.29065	19.43	0.3	0.069
C 2 - C 3	π	1.64062	C 4 - C 5	π^*	0.34593	18.55	0.29	0.065
C 2 - C 3	π	1.64062	C 10 - O 12	π^*	0.10479	18.37	0.28	0.069
C 3 - C 4	σ	1.97643	C 2 - C 3	σ^*	0.03265	3.68	1.27	0.061
C 3 - C 4	σ	1.97643	C 4 - C 5	σ^*	0.02630	3.57	1.28	0.06
C 4 - C 5	σ	1.97588	C 3 - C 4	σ^*	0.04641	3.55	1.26	0.06
C 4 - C 5	σ	1.97588	C 3 - O 18	σ^*	0.02624	3.54	1.07	0.055
C 4 - C 5	π	1.65861	C 1 - C 6	π^*	0.29065	17.05	0.3	0.065
C 4 - C 5	π	1.65861	C 2 - C 3	π^*	0.40550	21.69	0.29	0.072
C 5 - C 6	σ	1.97648	C 4 - O 13	σ^*	0.02720	4.01	1.05	0.058
C 5 - H 8	σ	1.97723	C 3 - C 4	σ^*	0.04641	4.36	1.07	0.061
C 6 - H 9	σ	1.98015	C 1 - C 2	σ^*	0.02157	3.61	1.09	0.056
C 10 - H 11	σ	1.98790	C 1 - C 2	σ^*	0.02157	3.74	1.1	0.057
C 10 - O 12	π	1.97971	C 2 - C 3	π^*	0.40550	5.01	0.4	0.044
C 19 - H 20	σ	1.98439	C 26 - C 27	σ^*	0.02437	3.52	1.1	0.056
C 19 - H 21	σ	1.98566	C 22 - C 27	σ^*	0.02454	3.84	1.1	0.058
C 22 - C 23	σ	1.97871	C 19 - C 27	σ^*	0.02203	3.6	1.12	0.057
C 22 - C 23	σ	1.97871	C 22 - C 27	σ^*	0.02454	3.27	1.28	0.058
C 22 - C 23	π	1.65930	C 24 - C 25	π^*	0.32817	20.65	0.28	0.068
C 22 - C 23	π	1.65930	C 26 - C 27	π^*	0.34952	20.71	0.29	0.069
C 22 - C 27	σ	1.97404	C 26 - C 27	σ^*	0.02437	3.57	1.27	0.06
C 22 - H 28	σ	1.97927	C 23 - C 24	σ^*	0.01616	3.62	1.1	0.056
C 22 - H 28	σ	1.97927	C 26 - C 27	σ^*	0.02437	4.58	1.1	0.063
C 23 - H 29	σ	1.98009	C 22 - C 27	σ^*	0.02454	3.65	1.09	0.056
C 23 - H 29	σ	1.98009	C 24 - C 25	σ^*	0.01617	3.66	1.1	0.057

Donors	Type of Bonds	Occupancy	Acceptors	Type of Bonds	Occupancy	Energy E(2) Kcal/mol	Energy Difference E(j)-E(i) a.u.	Polarized Energy F(i,j) a.u.
C 24 - C 25	π	1.65794	C 22 - C 23	π^*	0.31905	19.71	0.28	0.067
C 24 - C 25	π	1.65794	C 26 - C 27	π^*	0.34952	20.7	0.29	0.069
C 24 - H 30	σ	1.98004	C 22 - C 23	σ^*	0.01517	3.75	1.1	0.057
C 24 - H 30	σ	1.98004	C 25 - C 26	σ^*	0.01522	3.76	1.1	0.057
C 25 - C 26	σ	1.97867	C 19 - C 27	σ^*	0.02203	3.6	1.12	0.057
C 25 - H 31	σ	1.98015	C 23 - C 24	σ^*	0.01616	3.66	1.1	0.057
C 25 - H 31	σ	1.98015	C 26 - C 27	σ^*	0.02437	3.64	1.1	0.056
C 26 - C 27	σ	1.97395	C 22 - C 27	σ^*	0.02454	3.59	1.27	0.06
C 26 - C 27	π	1.65188	O 18 - C 19	σ^*	0.03864	6.47	0.5	0.055
C 26 - C 27	π	1.65188	C 22 - C 23	π^*	0.31905	20.38	0.28	0.068
C 26 - C 27	π	1.65188	C 24 - C 25	π^*	0.32817	20.15	0.28	0.067
C 26 - H 32	σ	1.97934	C 22 - C 27	σ^*	0.02454	4.58	1.1	0.063
C 26 - H 32	σ	1.97934	C 24 - C 25	σ^*	0.01617	3.61	1.1	0.056
O 12	n	1.88678	C 2 - C 10	σ^*	0.05952	18.09	0.71	0.102
O 12	n	1.88678	C 10 - H 11	σ^*	0.06069	21.54	0.64	0.106
O 13	σ	1.94885	C 3 - C 4	σ^*	0.04641	5.18	1.04	0.066
O 13	n	1.91981	C 4 - C 5	σ^*	0.02630	5.65	0.94	0.066
O 13	n	1.91981	C 4 - C 5	π^*	0.34593	5.83	0.4	0.046
O 13	n	1.91981	C 14 - H 16	σ^*	0.01731	5.46	0.75	0.058
O 18	σ	1.94970	C 3 - C 4	σ^*	0.04641	5.36	1.05	0.067
O 18	n	1.91509	C 2 - C 3	σ^*	0.03265	5.37	0.94	0.064
O 18	n	1.91509	C 2 - C 3	π^*	0.40550	7.07	0.4	0.052

Table 8: Details of the ligand-protein interaction

Protein (PDB ID)	No. of hydrogen bond	Bonded Residues	Bond Distance
2PG5	3	ILE 182	2.0
		THR 303	2.1
		GLY 302	3.2

IV. CONCLUSION

An anti-proliferative agent 2-benzyloxy-3-methoxybenzaldehyde (benzyl-o-vanillin) was fully characterized with different spectroscopic (FT-IR, FT-Raman, UV-Vis, ¹H and ¹³C NMR) approaches. DFT calculations were carried out on the same molecule and the data showed a good agreement with the experimental values. The structural parameters such as bond lengths and bond angles were calculated and compared with reported XRD results. Mulliken charges were analyzed and identified that positive and negative charges atoms (C2 and C3) are presented in benzaldehyde ring. NBO analysis reflects the charge transfer takes place within the molecule. HOMO and LUMO orbitals have been visualized and the energy gap between HOMO and LUMO supports the bioactivity property of the molecule. The MEP map shows the negative potential sites are on C=O atoms and the positive potential sites are around the hydrogen atoms. The molecular docking method was made with the protein of CYP2B5 substrate. It ensures that the results of this study may help researchers to go into the new insights of the compound in pharma field.

ACKNOWLEDGEMENTS

We remain grateful to Kanchi Mamunivar Center for Post Graduates studies, Lawspet, Puducherry for providing the Quantum Computational Research Lab for this study.

REFERENCES:

- [1] Mohammed Hadi Al-Douh, Shafida Abd. Hamid* and Hasnah Osman School of Chemical Sciences, Universiti Sains Malaysia (USM), Minden 11800.
- [2] Allen, F. H., Kennard, O., Watson, D. G., Brammer, L., Orpen, A. G. & Taylor, R. (1987). *J. Chem. Soc. Perkin Trans. 2*, pp. S1–19.
- [3] Scott, J. L. & Raston, C. L. (2000). *Green Chem.* 2, 245–247.
- [4] Berger et al., PhD Thesis, Virginia Polytechnic Institute and State University, Blacksburg, Virginia, USA J. M. (2001).
- [5] Jarrahpour, A. A. & Zarei, M. (2004). *Molbank*, pp. 377–378.
- [6] Devassy, B. M., Shanbhag, G. V., Lefebvre, F., Bohringer, W., Fletcher, J. & Halligudi, S. B. (2005). *J. Mol. Catal. A Chem.* 230, 113–119
- [7] Cotterill, A. S., Hartopp, P., Jones, G. B., Moody, C. J., Norton, C. L., O'Sullivan, N. & Swann, E. (1994). *Tetrahedron*, 50, 7857–7874
- [8] Mohammed H. Al-Douh, Shafida A. Hamid, Hasnah Osman, Shea-Lin Ng and Hoong-Kun Fun, *Acta Crystallographica Section E Structure Reports Online*, September 2006 DOI: 10.1107/S1600536806039250
- [9] Lin C-F, Yang J-S, Chang C-Y, Kuo S-C, Lee M-R. *Bioorg Med Chem* 13 (2005)1537-1544. doi:10.1016/j.bmc.2004.12.026. Pub-Med: 15698770.
- [10] M.J. Frisch et al., GAUSSIAN 09,

- Revision A.1, Gaussian, Inc., Wallingford, CT, 2009.
- [11] M.H. Jamroz, Vibrational Energy Distribution Analysis VEDA 4, Warsaw, 2004–2010.
- [12] A. Frisch, A.B. Nielson, A.J. Holder, GAUSSVIEW User Manual, Gaussian Inc., Pittsburgh, PA, 2000.
- [13] James J.P Stewart. model, 13(2007) 1173.
- [14] P.B. Nagabalasubramanian, S. Periandy, Mehmet Karabacak, M. Govindarajan, Spectrochimica Acta Part A: Molecular and Biomolecular Spectroscopy 145 (2015) 340–352.
- [15] Mohammed Hadi Al-Douh, Shafida Abd Hamid and Hasnah Osman, Indo. J. Chem., 2008, 8 (3), 411 – 417
- [16] P. F. Schatz, Laboratory Research Notebook A, page 13.
- [17] J. Mohan, Organic Spectroscopy—Principle and Applications, 2nd ed., Narosa Publishing House, New Delhi, 2004, pp. 30–32.
- [18] R.P. Hirschmann, et al., Spectrochim. Acta A 30 (1974) 1293.
- [19] B. Smith, Infrared Spectral Interpretation: A Systematic Approach, CRC Press, Washington, DC, 1999.
- [20] E.A. Nicol, et al., Spectrochim. Acta 30 (1974) 1717.
- [21] K. Jayasheela, S. Periandy, Journal of Molecular Structure 1159 (2018) 83–95.

* * * * *